2-Propanol Interacting with $Co_3O_4(001)$: A combined AIMD and vSFS study

Amir H. Omranpoor,[†] Anupam Bera,[†,§] Denise Bullert,[†] Matthias Linke,[†] Soma Salamon,[‡,¶] Samira Weber,[‡,¶] Heiko Wende,[‡,¶] Eckart Hasselbrink,[†,¶] Eckhard Spohr,[†] and Stéphane Kenmoe[*,†]

†*Fakultät für Chemie, Universität Duisburg-Essen, D-45117 Essen, Germany*

‡*Fakultät für Physik, Universität Duisburg-Essen, D-47057 Duisburg, Germany*

¶*Center for Nanointegration (CENIDE), Universität Duisburg-Essen*

§*present address: Institute of Physical Chemistry, Universität Jena, D-07743 Jena, Germany*

E-mail: stephane.kenmoe@uni-due.de

Abstract

The interaction of 2-propanol with $Co_3O_4(001)$ was studied by vibrational sum frequency spectroscopy (vSFS) and by ab initio molecular dynamics (AIMD) simulations of 2-propanol dissolved in a water film to gain insight at the molecular level into the pathways of catalytic oxidation. The experimental study has been performed under near ambient condition, where the presence of water vapor is unavoidable, resulting in a water film on the sample and thereby allowing us to mimic the solution-water interface. Both experiment and theory conclude that 2-propanol adsorbs molecularly. The lack of dissociation is attributed to the adsorption geometry of 2-propanol in which the O-H bond does not point towards the surface. Furthermore, the copresent water not only competitively adsorbs on the surface but also inhibits 2-propanol deprotonation. The

calculations reveal that the presence of water deactivates the lattice oxygen, thereby reducing the surface activity. This finding sheds light on the multifaceted role of water at the interface for the electrochemical oxidation of 2-propanol in aqueous solution as recently reported.[1] At higher temperatures 2-propanol remains molecularly adsorbed on Co_3O_4(001) until it desorbs with increasing surface temperature.

Introduction

Hydrocarbon oxidation catalyzed by mixed metal oxides is responsible for about 25% of the total production of industrial chemicals.[2] However, to describe chemical reactivity and selectivity at the surface, a detailed physical picture of molecular structure, composition and adsorption geometry is the first essential piece of information needed to further a deeper understanding. Extracting this information is difficult with conventional spectroscopic methods, due to the presence of relatively small number of chemical species at the interface when compared to those in the bulk. In operando, these problems are worsened by the interference with the background reactand solution. Therefore, to advance the understanding of reactivity and selectivity of catalysts ultimately allowing for a rational design, the initial mechanistic steps at the molecular level must be well understood and framed by appropriate surface specific experimental and theoretical models. Vibrational sum frequency generation spectroscopy (vSFS) is one of few techniques suited to obtain this kind of information from the sample interface because of its inherent surface selectivity. Thereby allowing us to gain direct insight into catalytic process.[3–6] In parallel, ab initio molecular dynamics (AIMD) simulations were performed to provide atomistic level insights to the experimental observations. It is expected that our study provides the foundation for a better understanding of 2-propanol oxidation on the Co_3O_4(001) surface in the presence of hydrated oxidants.

In this work, we study the interaction of 2-propanol with the Co_3O_4(001) transition metal oxide (TMO) surface. Over the years, substantial research effort has devoted to study the suitability of TMOs for their use as heterogeneous catalysts, mainly because of their

abundance and the resulting low cost compared to precious metal catalysts. Co_3O_4 spinel, in particular, has drawn significant attention since it promotes many oxidation reactions, one of the most important being the selective oxidation of hydrocarbons.[7–9] In addition, the various electronic, magnetic and redox properties of Co_3O_4 have also stimulated several studies in recent years.[10–15]

Falk et al.[1] studied the oxidation of 2-propanol over $Co_{1+x}Fe_{2-x}O_4$ spinel oxides in contact with both the liquid and the gas phase. They reported that increasing the Co content will increase the catalytic activity of the samples for 2-propanol oxidation, which shows that the iron-free Co_3O_4 samples have the highest catalytic activity. Moreover, their XPS analysis suggested that Co^{3+} sites are more active than Co^{2+} sites. Anke et al.[10] investigated the gas-phase oxidation of 2-propanol on Co_3O_4 nanoparticles. They found that Co_3O_4 spinel is a highly active and selective catalyst for the oxidation of 2-propanol, with the largest conversion rates of 2-propanol to acetone at temperatures between 373 and 573 K and the maximum around 430 K. Theoretical investigation in their study also showed that a Langmuir-Hinshelwood mechanism is preferred on the $Co_3O_4(001)$ surface.

Co_3O_4 nanospheres with a preferential (110) surface orientation were also studied by Falk et al.[16] They reported full conversion and 100% selectivity for 2-propanol oxidation to acetone at 430 K. In contrast to the theoretical finding for (001) surface orientation, they suggested a preferential Mars-van Krevelen mechanism for the (110) surface.[16] Recently, Roy and coworkers performed a DFT study of 2-propanol adsorption on strontium titanate (STO)[17] and found three geometries for molecular adsorption of rather similar binding energy.

The present manuscript is structured as follows. First, we present the results of the vSFS study that provides detailed information regarding chemical composition of the adsorbate layer and geometry of adsorbed molecule. Then, we discuss the pertinent analysis from a series of simulations of a $Co_3O_4(001)$ in contact with 2-propanol. These calculations allow us to gain some insight into the electronic structure at the interface and into the chemical dynamics of 2-propanol under operando conditions. We continue by discussing results at

elevated temperatures up to 450K.

Experimental Methods

Vibrational sum frequency spectroscopy rests on a non-linear optical process, the details of which were discussed in detail by several authors.[18,19] In brief, an IR light wave is mixed with a visible light beam when reflected at the interface in a way that produces a sum frequency beam that only carries information from the interfacial region. This process is particularly efficient if the IR wavelength matches a vibrational resonance in the adlayer such that tuning the IR light allows us to obtain the vibration spectrum. A scanning vSF spectrometer with approx. 12 cm^{-1} resolution was used (Ekspla PL2231 and PG501DFG) that utilizes wavelength tuneable IR pulses of 25 ps duration and 532 nm light pulses for upconversion at a repetition rate of 50 Hz. Pulse energies of 280 μJ (532 nm) and 10–30 μJ (IR) were applied. For every data point typically 300 laser pulses were sampled and averaged. In order to normalize the data with respect to day-to-day fluctuations in laser performance the reference signal from a Au sample was used.

The experimental set-up was described in detail elsewhere (Fig. 1).[3] The samples were mounted in a home-built compact cell (63 mm inner diameter) which allowed for the preservation of a rough vacuum before admitting 50 mbar of 2-propanol utilizing an evaporator to a nearly saturated alcohol atmosphere above the substrate surface. The laser beams enter and the signal leaves the cell through a MgF_2 window. The IR and upconversion light beams were directed at the sample under incident angles of 40° and 54° with respect to the surface normal, respectively. Before recording any spectra, the samples were further cleaned utilizing a two-stage cleaning process: *i*) exposure to an oxygen plasma (0.4 mbar, 15–30 min) and *ii*) in situ exposure to UV irradiation from a Xe lamp (Osram, XBO 150 W/1) in the presence of an oxygen atmosphere (100–200 mbar, 2–5 h).

Anhydrous 2-propanol (99.5%) was obtained from Sigma Aldrich and used without fur-

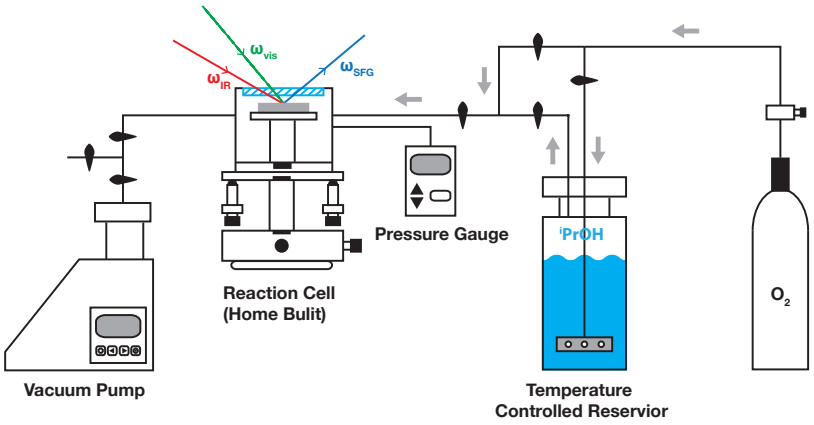

Figure 1: Experimental set-up. Alcohol is flown from a temperature controlled reservoir through the reaction cell which is evaporated by vacuum pump. The laser beams enter and the signal beam leaves the reaction cell through a MgF_3 window. A oxygen cylinder provides the gas for sample cleaning under UV light.

.

ther purification. 2-propanol-d6 was obtained from Cambridge Isotope Laboratories, Inc. (98%).

To fit the data, we used the following established expression[20,21]

$$I^{SFS}(\omega_{IR}) \propto \left| \left|\chi^{(2)}_{NR}\right| + \sum_i e^{i\xi_i} \frac{A_i}{\omega_{IR} - \omega_i + i\Gamma_i} \right|^2, \tag{1}$$

where $\chi^{(2)}_{NR}$ represents the 2$^{\text{nd}}$ order susceptibility of the substrate electronic system leading to a non-resonant background. A_i, ω_i and Γ_i are the vSF line strength, the position and the damping constant of the i^{th} vibrational resonance, respectively. ξ_i represents the relative phase of the vibrational contribution to the non-resonant susceptibility. ω_{IR} is the frequency of the incident IR light.

These parameters are real numbers and A_i has a positive value in our model. ξ_i is the relative phase of the response of each individual line with respect to the non-resonant background. For the *ssp* polarization combination, the phase difference of the responses of

symmetric stretches and anti-symmetric ones is π. For the *ppp* polarization combination that difference is treated as a fitting parameter.[22]

The surface density of an adsorbed species N_i can be inferred from the A_i values derived from the fit to a spectrum as they are connected according to the following expression[23]

$$A_i = N\langle a_i \rangle_f = N_i \int a_i \, f(\Omega) \, d\Omega, \tag{2}$$

where a_i is the non-linear molecular hyperpolarizability strength for the combination of light polarizations used in the experiment associated with the i^{th} vibrational resonance, and $\langle \, \rangle_f$ indicates an average with respect to the orientational distribution function $f(\Omega)$ with Ω denoting the set of three Euler angles.

The Co_3O_4(001) sample was grown on a MgO(001) substrate by pulsed laser deposition using a custom-built UHV system with a base pressure of 2x10^{-8} mbar. Prior to the deposition, the substrate was heated to 300 °C, followed by the introduction of a constant flow of neat O_2 into the chamber via a precision valve until a stable pressure of 1.7x10^{-2} mbar was reached. A 248 nm excimer laser (Coherent COMPexPro 102) was used to ablate from a CoO Target (MaTecK) with a pulse energy of 200 mJ and a frequency of 10 Hz. The deposition rate at these settings was previously determined with a quartz crystal microbalance positioned at the substrate position to be 2.3 Å/s. Following the deposition, the substrate was annealed at 400 °C for 45 minutes in a neat O_2 atmosphere. Furthermore, the morphology and crystallinity were characterized by atomic force microscopy (AFM) and X-ray diffaction (XRD), respectively, and are further discussed in the supporting information.

Computational Methods

A Co_3O_4 crystal can be cleaved in two ways along the (001) direction to form a so-called A-terminated surface (which contains both Co^{2+} and Co^{3+} ions in the topmost layer) and a B-terminated surface (where the topmost layer consists only of Co^{3+} ions). For further

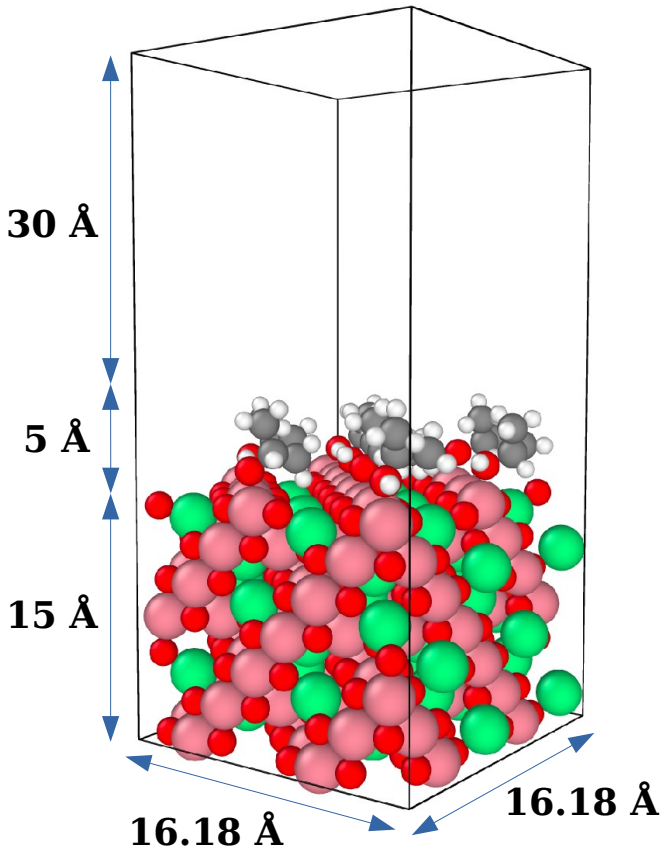

Figure 2: 2-propanol adsorbed on the B-terminated Co_3O_4(001) surface. Co^{3+} (pink), Co^{2+} (green), O (red), C (gray) and H (white).

details on the differences between these two terminations and their interactions with water the reader is referred to a recent publication.[24] In the present study, however, we focus on B-termination, since the experimental samples showed behavior more characteristic of B-termination, as will be discussed below. Figure 2 shows the simulation box for the case of B-terminated Co_3O_4(001) interacting with 2-propanol molecules.

The Co_3O_4 (001) slabs used in the present work form an orthorhombic supercells with 2×2 periodicity in the lateral directions (x, y). As a result, the dimensions of the samples in these directions are equal to 16.18 Å × 16.18 Å. The crystal slab with B-termination on both sides consists of 13 layers and is thus non-stoichiometric. This choice was made to reduce the electric field in the vacuum region. Atoms in the bottom 6 slab layers were kept

immobile in order to mimic bulk behavior. A dipole correction as described in Ref.[25] was used in the z direction to cancel out the impact of the asymmetry caused by the difference between the constrained and unconstrained surfaces of the slab and also in view of the fact that 2-propanol is adsorbed only on the top side of the slab. Eight 2-propanol molecules were added to the system so as to cover the cobalt oxide surface. A vacuum region of about 30 Å thickness above the adsorbate film in the z direction was devised, in order to avoid artificial interactions between the upper and the lower surface of the $Co_3O_4(001)$ samples due to periodic boundary conditions, which were applied in all three directions of space.

Born-Oppenheimer Molecular Dynamics simulations, as implemented in the CP2K/Quickstep package,[26] were performed at the Γ point. Density functional theory (DFT) was employed for describing the electronic structure. The PBE functional[27] was utilized to treat exchange and correlation effects, and a U correction of the Hubbard[28] type was added to achieve a correct description of Co $3d$ states. The value of U which was taken from our previous studies[24,29–33] and set to 2 eV. In order to take into account the dispersion interactions, specifically in the water films, the Grimme D3 correction was added to the PBE exchange-correlation functional.[34] The core electrons were described by Goedecker-Teter-Hutter (GTH) pseudopotentials. The $2s$ and $2p$ electrons of O and C atoms, and the $3s$, $3p$, $3d$ and $4s$ electrons for Co atoms were explicitly treated as valence electrons. The mixed-representation basis sets consisted of plane waves with an energy cutoff of 500 Ry and a double-ζ quality local basis set with a single set of polarization functions (DZVP).

The MD simulations were performed in the canonical ensemble using a Nosé-Hoover thermostat with a time constant of 1 ps and target temperatures of 300 K and 450 K. After an equilibration time of approximately 1 ps, the simulations were run for a production phase of about 20 ps, using a simulation time step of 0.5 fs.

Experimental Results and Discussion

The pristine Co_3O_4 surface is known to be very reactive towards water vapor,[24] and thus under rough vacuum conditions one is to expect preadsorption of water and hydroxylation of the surface from the residual gas as H_2O dissociates over oxygen defect sites. The consequences for the vSFS were discussed by some of us in the context of methanol interacting with TiO_2.[3] Similarly, for Co_3O_4 a broad featureless signal is observed in the H-bonded OH region between 3100 and 3450 cm^{-1} (Fig. 3). It is understandable that the OH-band is broad, due to the coexistence of different binding sites on $Co_3O_4(001)$ and the formation of a hydrogen bonded network with adsorbed water. This observation raises the question of whether hydroxylation of the surface will decrease the surface catalytic activity by deactivating surface lattice oxygen. No significant change of the spectrum in the OH region is observed after admitting 50 mbar of 2-propanol into the vacuum cell suggesting that the OH is not significantly displaced. In the region of the C-H stretching vibrations at 2850 – 2980 cm^{-1} several features are observed which are superimposed on the non-resonant background.

Figure 4 displays the vSF spectra obtained for $Co_3O_4(001)/MgO(001)$ exposed to 50 mbar of 2-propanol at room temperature utilizing all three useful polarization combinations of the light beams denoted as *ppp*, *ssp* and *sps*. This nomenclature denotes the polarizations of the reflected SF signal, and the incident visible and IR light pulses, in that order, with respect to the plane of incidence. The vSF spectrum of 2-propanol in the C-H stretching region was discussed by us before when studying its interaction with TiO_2.[4] The observed features are consistent with earlier detailed Raman studies.[35] With increasing alkyl chain length, the spectra of alcohols become congested as a larger number of modes need to be considered, which often overlap and for which multiple Fermi resonances have to be expected. However, in the *sps* spectrum only the anti-symmetric stretching mode, r^-, at 2980 cm^{-1} is vSF active for symmetry reasons. In line with this argument, the r^- modes will not appear in the *ssp* spectrum. Instead, two symmetric modes, r^+ and a related Fermi resonance with the overtone of the degenerated bending mode, r^+_{FR}, at 2888 and 2945 cm^{-1} are clearly visible.

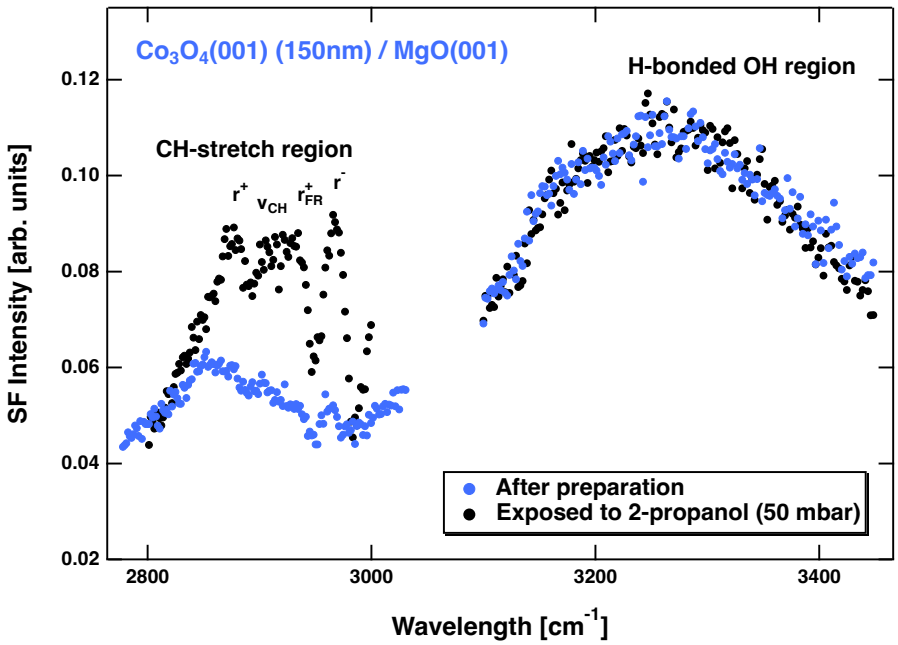

Figure 3: vSF spectra of a $Co_3O_4(001)$/ MgO(001) surface obtained using the *ppp* polarization combination in the hydrogen-bonded OH as well as CH stretch region prior to dosing any 2-propanol and after admitting 50 mbar of 2-propanol.

Moreover, methine contributes with a number of modes located between 2850 and 2935 cm^{-1} identified by us in a previous study when discussing 2-propanol-d6 spectra.[4] In the fit to the spectra reported here, we transferred the wavenumber and ratio of intensities of these features from the earlier study in view of the noise int he data. Hence, only two free parameters, an amplitude factor and the phase, are left. In the *ppp* polarization spectrum the largest number of bands is observed: namely, the CH_3 symmetric stretch, r^+, at 2884 cm^{-1}, as well as r^+_{FR}, at 2944 cm^{-1}, the CH_3 anti-symmetric stretch, r^-, at 2978 cm^{-1}, and the methine modes just discussed. Their positions were also inferred from the previous report. We found that fitting is complicated by the fact that the "non-resonant" background has some very broad structure. Namely, the intensity is by a factor of 2 larger at the high wavenumber end of the spectrum. All the positions (for a compilation of fitting parameters and further details see the SI) agree well with what we reported earlier for 2-propanol interacting with TiO_2.[4] It is important to note here that the spectra are strongly influenced by a *nonresonant* background, which originates from the tail of the broad feature due to H-bonded OH

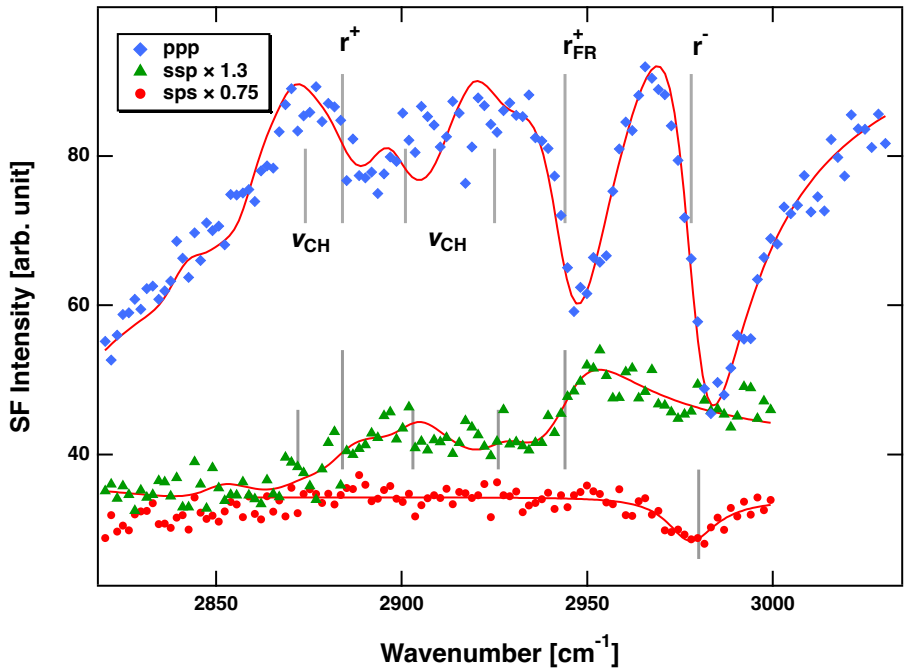

Figure 4: vSF spectra of a $Co_3O_4(001)$/ MgO(001) surface exposed to 50 mbar of 2-propanol for the *ppp*, *ssp* and *sps* polarization combinations. The vertical bars mark the center positions of the bands identified. The shorter ones correspond to the features observed earlier in a 2-propanol-d6 spectrum.

groups, and which interferes with the molecular resonances in a coherent spectroscopy such as vSFS. We discussed this in detail earlier.[3] Taking all these findings into account, overlapping resonances and mutual interference produce the observed non-Lorentzian line shapes. Therefore, the center frequencies of the C-H stretching modes marked in Fig. 4 do not necessarily coincide with maxima in the vSF spectrum. The discrepancies of 2 - 3 cm^{-1} between the line positions of the spectra taken using different polarization combinations reflect the experimental uncertainties.

It is most important to note that the spectrum can very well be fitted without the need to assume that a fraction of the adsorbate is deprotonated. This observation is similar to our previous finding for TiO_2 thin films.[4] The spectrum of the deprotonated species generally exhibits a red shift of all modes by about 20-30 cm^{-1} as it was observed on $SrTiO_3$ and $CeO_2(100)$.[5,6] In particular, a feature at about 2850 cm^{-1} would be expected to arise from adsorbed 2-propoxy groups. The small shoulder in the *ppp* spectrum at this wavenumber

is not assigned to the deprotonated species because also the earlier 2-propanol-d6 spectrum exhibited this bump. Hence, the lack of this spectral signatures suggests that the extent of deprotonation of 2-propanol is too small to be detected by our experiment. We thus conclude that 2-propanol adsorbs molecularly on Co_3O_4. However, note that our system is characterized by the presence of water and hydroxylation prior to exposure to 2-propanol, which sets it apart from earlier studies for other TMOs such as STO(100) and CeO_2(100).[5,6] In light of this conclusion, one may ask why deprotonation was not observed at room temperature and whether an energetic barrier for deprotonation may be overcome when the substrate temperature is raised. Little is known for the system studied here, but for ethanol on rutile TiO_2(110) the energy barrier for 0-H dissociation has estimated as 0.3 eV.[36]

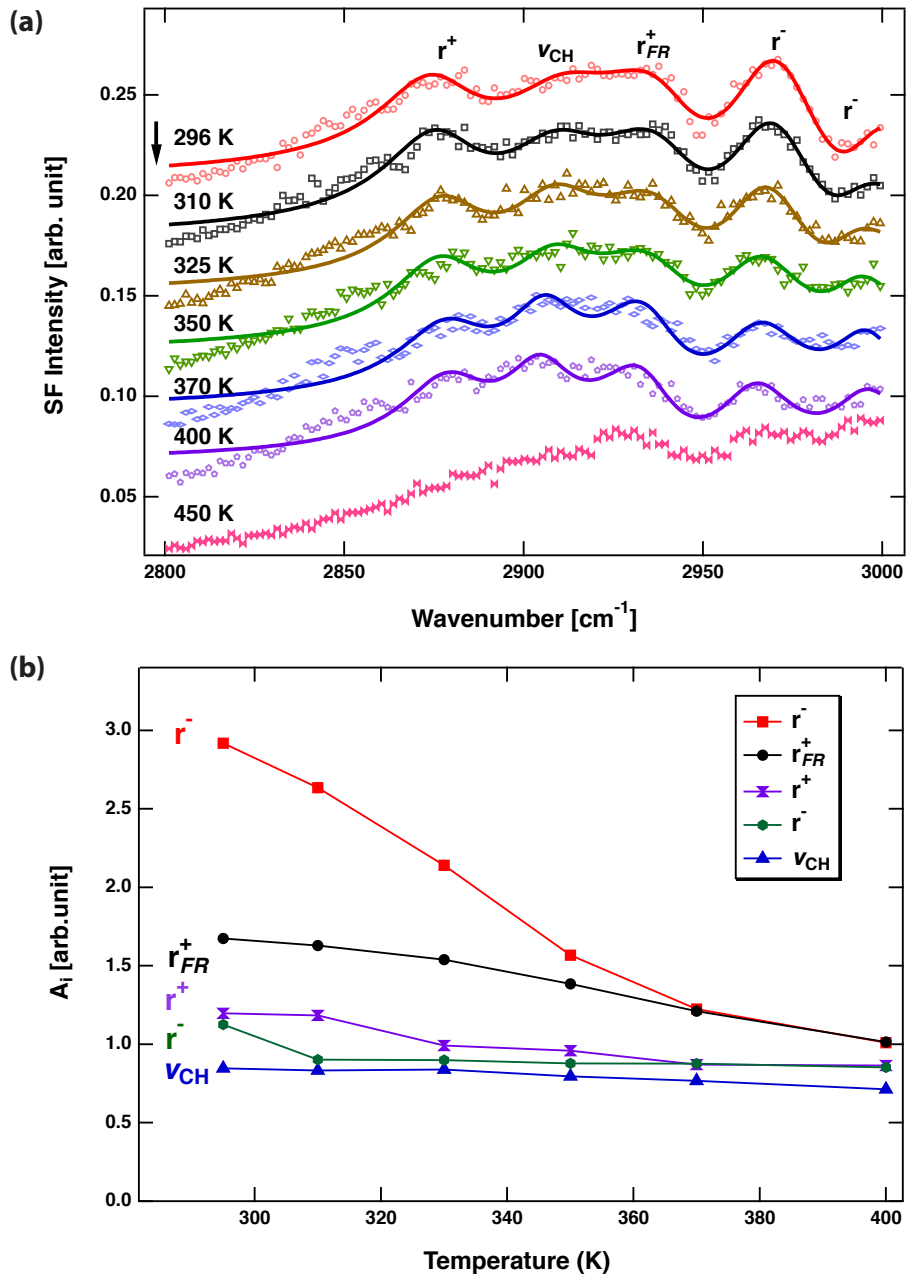

Figure 5: (a) Evolution of the vSF spectra of a $Co_3O_4(001)$/ MgO(001) surface exposed to 50 mbar of 2-propanol with temperature. Spectra were obtained using the *ppp* polarization combination. The curves were vertically offset to ease the access to the data. (b) Calculated oscillator strengths (A_i) derived from fitting the spectra for the four band identified. The data suggest that the molecular coverage of 2-propanol decreases with increasing temperature over the temperature range from 280 to 400 K before it completely vanishes at 450 K.

To address this question, a systematic study of the temperature dependence of spectra has been performed (Figure 5 (a)). Even at higher temperatures, there is no evidence of dissociation, since no new peak appears at lower wavenumbers.

While the vSF spectra are utilized to identify the adsorbed species, the number density can be derived from the oscillator strength obtained by fitting, provided that the adsorption geometry does not significantly change with temperature. This assumption is supported by the AIMD simulations (see below), which suggest a near-constant average orientation of the OH groups over the studied temperature range. The other parameters, (ω_i and Γ_i), were held constant when fitting the data, and the spectra can directly be compared. Fig. 5 (b) displays the oscillator strengths, A_i for the various modes. The data suggest that the density of molecular 2-propanol decreases with increasing temperature as there is a systematic decrease in the A_i values for the r^+, r^+_{FR} and r^- modes for temperatures up to 400 K. And at about 450 K most adsorbed species have desorbed altogether.

Having reliably assigned the bands in the SFG spectrum, the extracted amplitudes in the different polarization directions can be used to calculate the orientation of the 2-propyl functional group at the interface. The direction of the OH-bond, however, remains inaccessible.

To derive the adsorption geometry of the 2-propyl functional group with respect to the macroscopic surface normal we followed Kataoka and Cremer[37] and Doughty *et al.*[5] (s. SI for details). This procedure allows one to derive from the set of spectra for different polarization combinations the direction of the vector bisecting the two methyl groups with respect to the surface normal, 37°, and the twist angle around that vector, 29°, yielding the direction for the methine CH-bond. By also taking the molecular geometry into account one obtains the angle of the CO-bond with respect to the surface normal as 154°. This implies that one of the two methyl groups is positioned somewhat closer to the surface than the other. It is noteworthy that the experiment is only able to provide an average value based on the assumption of a single-modal Gaussian distribution within an azimuthally isotropic sample.

The simulation results seem to support the validity of this assumption (see below).

Computational Results

For the ideal $Co_3O_4(001)$ surface two terminations are possible: the A-termination (with a mixture of coordinatively unsaturated Co^{2+} and Co^{3+} ions in the top layer) and the B-termination (only undercoordinated Co^{3+} ions at the surface). Based on our previous work,[29] where we observed that the B-terminated surface is more active for electrochemical oxidation of 2-propanol, we chose here to study only the B-terminated Co_3O_4 surface. Additional support for this choice comes from recent experimental studies,[1] which also reported the predominance of Co^{3+} adsorption sites, characteristic for a B-terminated surface.

For the present study, we performed and analysed four different systems: *(i)* a perfect B-terminated $Co_3O_4(001)$ surface covered by 8 2-propanol molecules at 300 K (in the following denoted as S1); *(ii)* the same system at 450 K (S2), *(iii)* a "hydroxylated" system, where one extra hydrogen was placed next to one of the alcohol molecules, producing a surface OH group (S3); and *(iv)* a surface with a single 2-propanol molecule immersed in a film of 60 water molecules at 300 K (S4). Figure 6 shows top and side views of the room temperature system with 8 adsorbed molecules without (S1; left) and with (S3; right) the extra hydrogen atom, which is marked by an orange circle. In none of the four simulations did we observe any oxidation reaction, and only one alcoholic OH group dissociated in simulation S1 during the 20 ps simulation time. The thermally induced disorder of the adsorbed molecules is visible in all snapshots. It is also evident that the extra hydrogen atom forming the surface hydroxyl group has no strong effect on the surrounding 2-propanol.

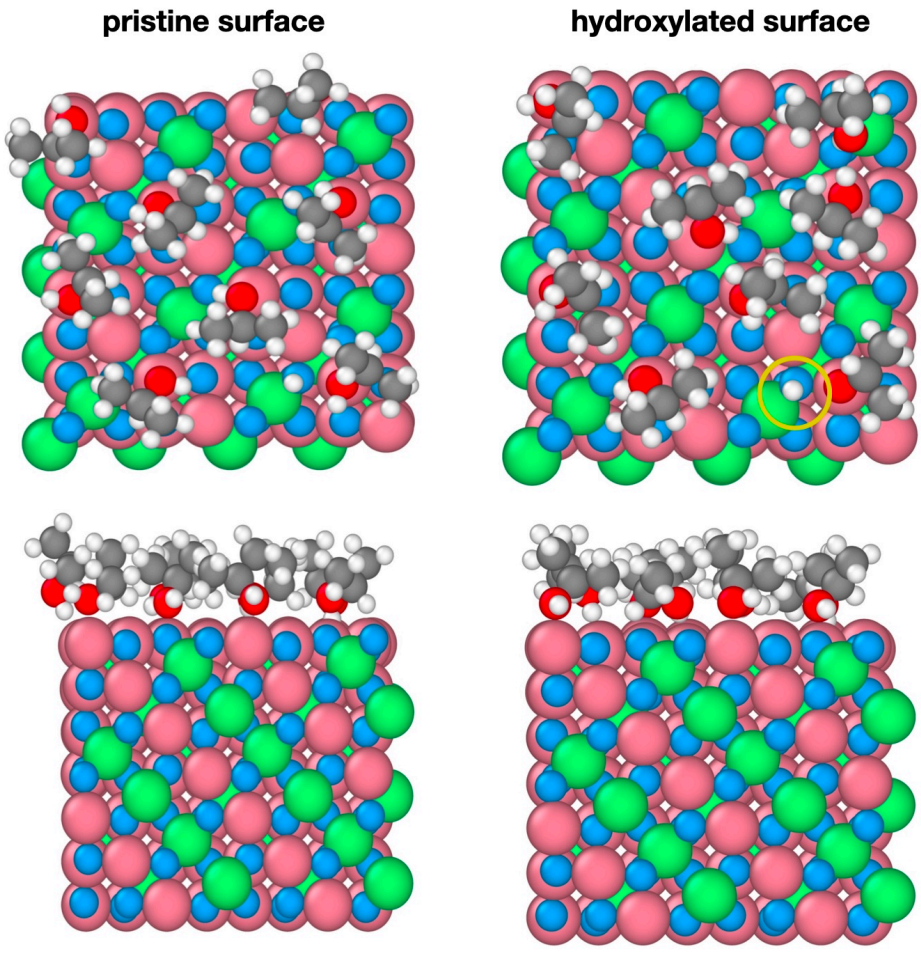

Figure 6: Top and side view snapshots from the pristine surface MD simulation S1 (left) and the hydroxylated surface simulation S3 (right). Both simulations of the B-terminated $Co_3O_4(001)$ surface were performed at 300 K; in the top right frame the extra hydrogen atom is indicated by a circle. Co^{3+} (pink), Co^{2+} (green), O in Co_3O_4 (blue), O in 2-propanol (red), C (gray) and H (white).

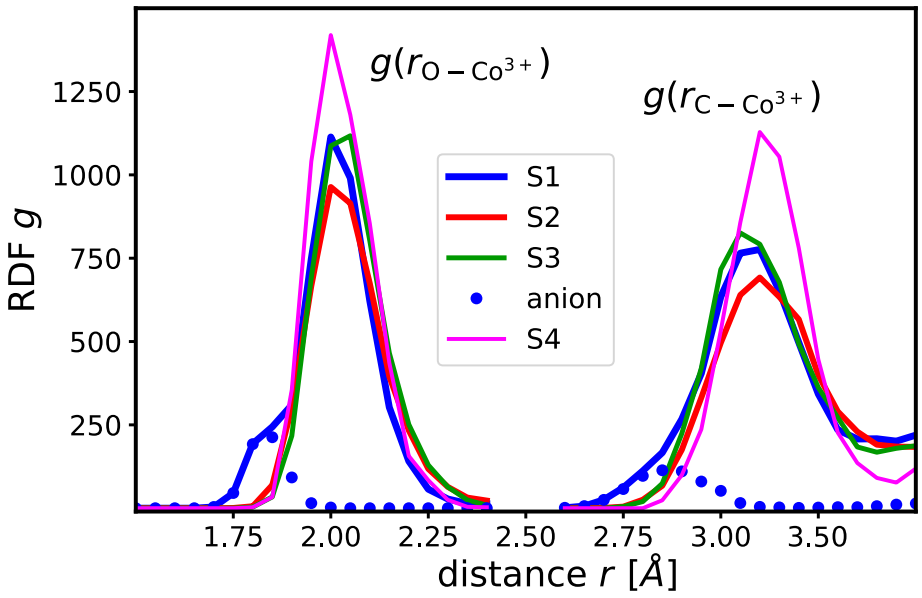

Figure 7: Radial distribution functions (RDFs) $g(r_{O-Co^{3+}})$ (left) and $g(r_{C-Co^{3+}})$ (right) as a function of distance r.

Binding of adsorbed 2-propanol molecules occurs through the oxygen atom, as can be seen by comparing the distances of the first peaks of the O-Co^{3+} and the C-Co^{3+} radial distribution functions (RDF) depicted in Fig. 7. Note that the values of the RDFs in simulation S4 are scaled by a factor of 8 in order to make peak heights easily comparable. The dotted graphs are for the subset of molecules in the anionic state, i.e., where the hydroxyl proton has been dissociated, and are *not* scaled. One can note that for simulation S4 the scaled peaks are somewhat higher and narrower than for simulations S1 and S3, which are very similar. Thus, the interaction between co-adsorbed 2-propanol molecules leads to less favorable orientations on the surface than for the isolated molecule dissolved in a water film (S4). As expected from the snapshots, the presence of the additional hydrogen atom in simulation S3 plays no significant role. Increasing the temperature from 300 K to 450 K broadens both the oxygen and the carbon peaks even more due to increased thermal motion. Upon deprotonation of 2-propanol the corresponding binding distances become shorter (circles and low-distance shoulders in the the S1 curves).

Figure 8 shows the orientational distribution of the C-O (top) and the O-H bond (bottom), which are both not directly accessible from the experimental data. One first notes that the orientational distribution for the single hydrated 2-propanol molecule (S4) is sharper than for the other systems, which is most likely a consequence of structural heterogeneity. The average angle of the C-O bond relative to the surface normal is about 130° for simulation S4 and between 120 and 125° for the remaining cases, indicating that the CO bond points towards the surface, consistent with the shorter $O - Co^{3+}$ distances in comparison to the $C - Co^{3+}$ distances in Fig. 7. Similarly, the OH distribution is also broader for the 2-propanol film simulations (S1-S3) when compared with the dissolved single-molecule case (S4). The O-H vector points slightly away from the surface in simulation S4 (at an average angle of about 82°). For the film simulations, two pronounced maxima are visible, with the preferred orientations being around 80-100°. The second maximum corresponds to molecules for which the O-H vector points towards the surface, which may represent early stages of molecules that eventually undergo dissociation into surface O-H groups and 2-propanolate anions.

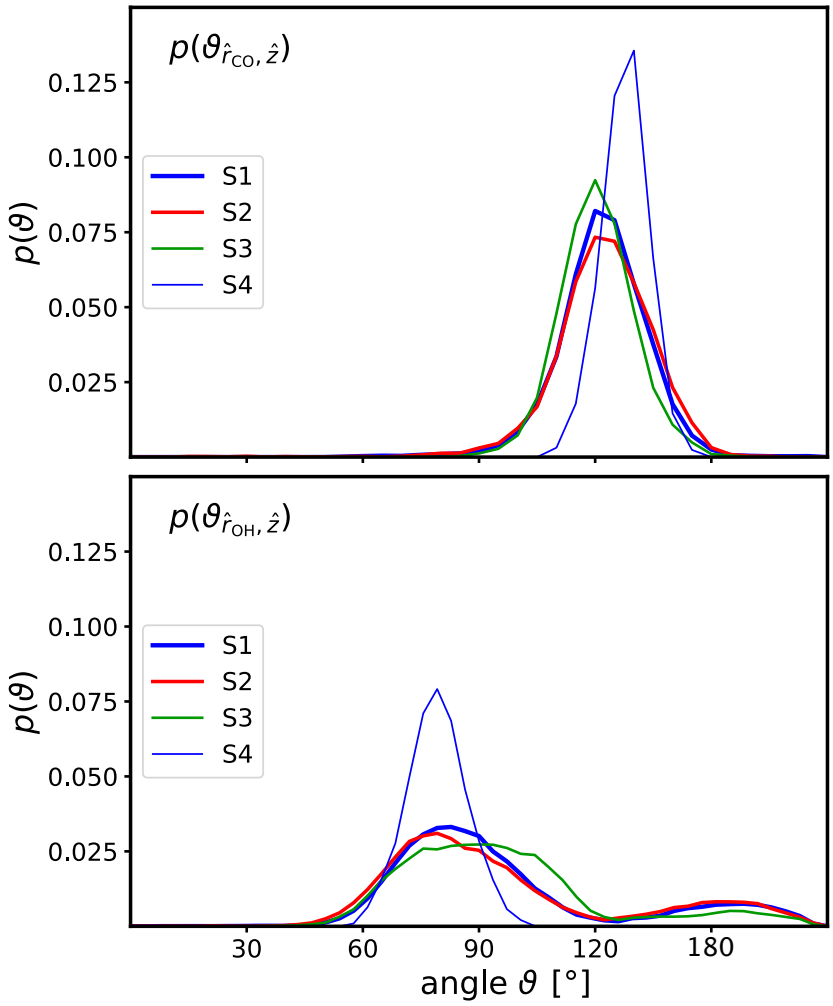

Figure 8: Distribution p of the angles ϑ between the surface normal $\hat{z}$ and the C-O unit vector $\hat{r}_{CO}$ (top) and the O-H unit vector $\hat{r}_{OH}$ (bottom) of 2-propanol molecules.

To provide the basis for comparison with the experimental evidence, Fig. 9 shows the joint distribution function of providing a specific tilt angle of the CCC angle bisector relative to the surface normal (along the horizontal axis) and a specific $C_{CH_3} - C_{CH_3}$ vector between the two methyl groups and the surface normal (along the vertical axis). When the tilt angle is smaller than 90°, the methyl groups are further away from the surface as both the secondary carbon and the alcoholic oxygen atom and, consequently, the C-O bond points towards the surface at an angle, as visible in Fig. 8. Note that the second angle is an axial vector, i.e. its distribution is symmetric about the configuration where both methyl groups have the same distance from the surface at 90°. For all simulations one observes a clear maximum around 30± 20° for the tilt angle and about 60±20° for the C-C vector. Thus, the average prevailing molecular arrangement is one with a tilted CCC bisector and the two methyl groups slightly asymmetric relative to the surface. In simulation S4 this is the only configuration observed. In the remaining simulations, an additional maximum is observed around (90°, 90°), which is compatible with the minority O-H distributions around 150° in Fig. 8. This maximum, as more detailed analysis shows, is due to both static heterogeneity, i.e. over the course of the simulation most molecules accept these particular configurations, but with relatively low probability. An interesting case is depicted in the two rightmost graphs for the single molecule that dissociates during the course of the simulation in S1. It is evident that the molecule shifts from the prevailing configuration at (30°, 60°) in the undissociated state to the new one at (90°, 90°) after dissociation.

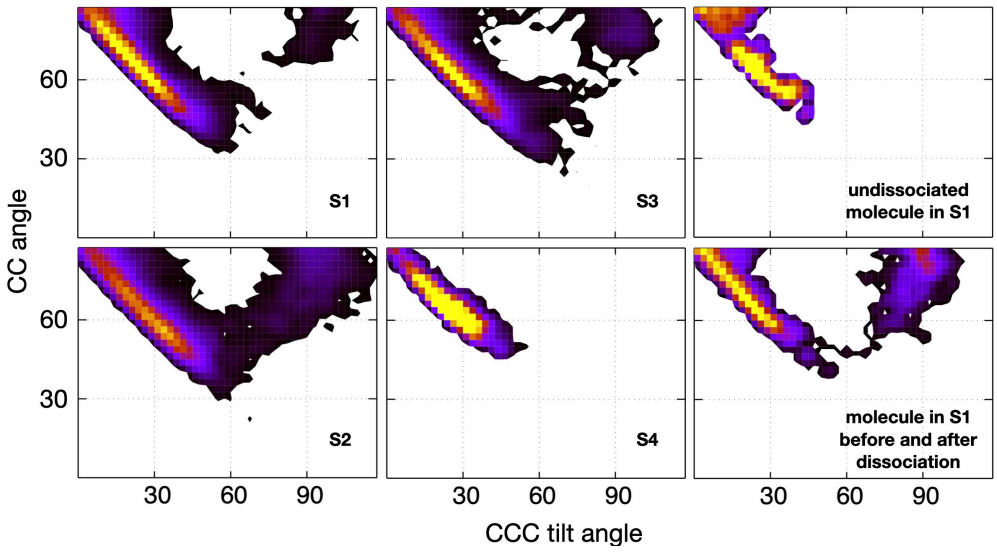

Figure 9: Joint distribution of tilt angles (the angle between the CCC bisector and the surface normal) and the angle between the $C_{CH_3} - C_{CH_3}$ vector and the surface normal for all molecules in all simulations. The two rightmost graphs show the behavior of the single dissociating molecule before dissociation (top) and for the entire simulation (bottom).

Conclusion

We have utilized vSFS experiment and AIMD simulation in order to study 2-propanol adsorption on the $Co_3O_4(001)$ surface. Furthermore, both experiment and theory agree on the fact that 2-propanol is almost exclusively molecularly adsorbed on the surface. Both approaches also agree that a temperature increase does not change adsorption properties significantly and in particular does not lead to large extent of deprotonation. In addition to surfaces covered by 2-propanol films, we also studied in AIMD simulations the behavior of a single hydrated 2-propanol molecule and a surface with a single extra hydroxyl group, the latter study being motivated by the experimental finding that preadsorbed OH groups are not displaced upon 2-propanol dosing. In the AIMD simulations, only a single event of dissociation of the alcoholic proton to form a surface OH bond was observed for 25 different molecules when lumping all simulations together.

From the experimental spectra, it was inferred that the tilt angle of the CCC angle bisector is about 30° from the surface normal, resulting in a deduced orientation of the CO vector to be about 140° from the surface normal. Hence, experimentally the CO vector should point towards the surface at an angle of about 40°. The simulation results also favor a similar orientation of the CO vector with, however, a larger angle of about 60° for the 2-propanol films and 50° for the solvated single 2-propanol. Both experiment and theory also agree on the fact that the preferred configurations show a slight asymmetry of the methyl surface distances with one distance slightly smaller than the other. While the experimental data do not provide any information about the orientation of the OH bond relative to the surface normal, the AIMD simulations show that the OH vector points more or less parallel to the surface for the film simulations and even slightly away for the single solvated 2-propanol molecule. However, in the film simulations we also find a minority population of configurations where the OH vector points relatively straight towards the surface. These configurations appear to be related to possible (but rare) dissociation steps.

Overall, simulation results and experimental analysis agree qualitatively, with minor

systematic quantitative differences in term of average orientations. Furthermore, simulation also strongly supports the assumption of a Gaussian distribution around a single preferential structure underlying the experimental data treatment. However, the simulated distributions are quite broad with full width at half maximum of typically about 30°, which indicates wide angle hindered rotations and suggests that focusing in the discussion on definite binding angles such as obtained from total energy calculations is not appropriate. Nevertheless, in conclusion, the combined experimental and theoretical picture supports a view of molecular adsorbed 2-propanol molecules with a preferential orientation where the CO bond point towards the surface at an angle and the where the CCC bisector vector points away from the surface.

Both experiment and simulation conclude that 2-propanol predominantly stays intact when interacting with $Co_3O_4(001)$. The lack of deprotonation to form surface OH and 2-propoxy is attributed to the adsorption geometry in which the O-H bond does not point towards the surface. The calculations reveal that hydroxylation as to be expected in the presence of water deactivates the lattice oxygen, thereby reducing the surface activity. As these conclusion seem in part to contradict the experimental reports of good catalytic activity, further studies in particular addressing less ideal surface structures are necessary to obtain a complete picture.

Acknowledgement

This work was funded by the Deutsche Forschungsgemeinschaft (DFG, German Research Foundation) – Project-ID 388390466 – CRC/TRR 247 "Heterogeneous Oxidation Catalysis in the Liquid Phase." Support by the Interdisciplinary Center for Analytics on the Nanoscale (ICAN) of the University of Duisburg-Essen, a DFG funded core facility (DFG resources reference: RI_00313, project nos. 233512597 and 324659309), is gratefully acknowledged. We thank Steffen Franzka for AFM characterization of the $Co_3O_4(001)$/ MgO(001) substrate.

Supporting Information Available

Atomic force microscopy images of a typical sample surface (Fig. S1 - S2), XRD characterization (Fig. S3) and details to the analysis of the vSF spectra.

References

(1) Falk, T.; Budiyanto, E.; Dreyer, M.; Pflieger, C.; Waffel, D.; Büker, J.; Weidenthaler, C.; Ortega, K. F.; Behrens, M.; Tüysüz, H., et al. Identification of Active Sites in the Catalytic Oxidation of 2-Propanol over $Co_{1+x}Fe_{2-x}O_4$ Spinel Oxides at Solid/Liquid and Solid/Gas Interfaces. *ChemCatChem* **2021**, *13*, 2942–2951.

(2) Grasselli, R. K. Fundamental principles of selective heterogeneous oxidation catalysis. *Topics in Catalysis* **2002**, *21*, 79–88.

(3) Bera, A.; Bullert, D.; Hasselbrink, E. Vibrational sum frequency spectroscopy study of methanol adsorption on thin film TiO_2 at ambient pressure and temperature. *J. Phys. Chem. C* **2020**, *124*, 16069–16075.

(4) Bera, A.; Bullert, D.; Linke, M.; Hasselbrink, E. Vibrational Sum Frequency Spectroscopy Study of Alcohol Adsorption on Thin-Film TiO_2 at Ambient Pressure and Temperature. *J. Phys. Chem. C* **2021**, *125*, 7721–7727.

(5) Doughty, B.; Srinivasan, S. G.; Bryantsev, V. S.; Lee, D.; Lee, H. N.; Ma, Y.-Z.; Lutterman, D. A. Absolute molecular orientation of isopropanol at Ceria(100) surfaces: Insight into catalytic selectivity from the interfacial structure. *J. Phys. Chem. C* **2017**, *121*, 14137–14146.

(6) Tan, S.; Gray, M. B.; Kidder, M. K.; Cheng, Y.; Daemen, L. L.; Lee, D.; Lee, H. N.; Ma, Y.-Z.; Doughty, B.; Lutterman, D. A. Insight into the selectivity of isopropanol

conversion at strontium titanate (100) surfaces: a combination kinetic and spectroscopic study. *ACS Catalysis* **2017**, *7*, 8118–8129.

(7) Waidhas, F.; Haschke, S.; Khanipour, P.; Fromm, L.; Görling, A.; Bachmann, J.; Katsounaros, I.; Mayrhofer, K. J.; Brummel, O.; Libuda, J. Secondary Alcohols as Rechargeable Electrofuels: Electrooxidation of Isopropyl Alcohol at Pt Electrodes. *ACS Catalysis* **2020**, *10*, 6831–6842.

(8) Hill, C. K.; Hartwig, J. F. Site-selective oxidation, amination and epimerization reactions of complex polyols enabled by transfer hydrogenation. *Nat. Chem.* **2017**, *9*, 1213–1221.

(9) Finocchio, E.; Willey, R. J.; Busca, G.; Lorenzelli, V. FTIR studies on the selective oxidation and combustion of light hydrocarbons at metal oxide surfaces Part 3.—Comparison of the oxidation of C_3 organic compounds over Co_3O_4, $MgCr_2O_4$ and CuO. *J. Chem. Soc., Faraday Trans.* **1997**, *93*, 175–180.

(10) Anke, S.; Bendt, G.; Sinev, I.; Hajiyani, H.; Antoni, H.; Zegkinoglou, I.; Jeon, H.; Pentcheva, R.; Roldan Cuenya, B.; Schulz, S., et al. Selective 2-propanol oxidation over unsupported Co_3O_4 spinel nanoparticles: mechanistic insights into aerobic oxidation of alcohols. *ACS Catalysis* **2019**, *9*, 5974–5985.

(11) Doheim, M.; El-Shobaky, H. Catalytic conversion of ethanol and iso-propanol over ZnO-treated Co_3O_4/Al_2O_3 solids. *Colloids and Surfaces A* **2002**, *204*, 169–174.

(12) Yang, T.; Kastenmeier, M.; Ronovskỳ, M.; Fusek, L.; Skála, T.; Waidhas, F.; Bertram, M.; Tsud, N.; Matvija, P.; Prince, K. C., et al. Selective electrooxidation of 2-propanol on Pt nanoparticles supported on Co_3O_4: an in-situ study on atomically defined model systems. *J. Phys. D* **2021**, *54*, 164002.

(13) Anke, S.; Falk, T.; Bendt, G.; Sinev, I.; Haevecker, M.; Antoni, H.; Zegkinoglou, I.; Jeon, H.; Knop-Gericke, A.; Schlögl, R., et al. On the reversible deactivation of cobalt

ferrite spinel nanoparticles applied in selective 2-propanol oxidation. *J. Catal.* **2020**, *382*, 57–68.

(14) Kenmoe, S.; Douma, D. H.; Raji, A. T.; M'Passi-Mabiala, B.; Götsch, T.; Girgsdies, F.; Knop-Gericke, A.; Schlögl, R.; Spohr, E. X-ray Absorption Near-Edge Structure (XANES) at the O K-Edge of Bulk Co_3O_4: Experimental and Theoretical Studies. *Nanomaterials* **2022**, *12*, 921.

(15) Douma, D. H.; Nchimi Nono, K.; Omranpoor, A. H.; Lamperti, A.; Debernardi, A.; Kenmoe, S. Probing the local environment of active sites during 2-propanol oxidation to acetone on the $Co_3O_4(001)$ surface: insights from first principles O K-edge XANES spectroscopy. *ChemRxiv* **2022**,

(16) Falk, T.; Anke, S.; Hajiyani, H.; Saddeler, S.; Schulz, S.; Pentcheva, R.; Peng, B.; Muhler, M. Influence of the particle size on selective 2-propanol gas-phase oxidation over Co_3O_4 nanospheres. *Catal. Sci. Technol.* **2021**, *11*, 7552–7562.

(17) Chapleski, R.; Chowdhury, A. U.; Mason, K. R.; Sacci, R. L.; Doughty, B.; Roy, S. Interfacial acidity on the strontium titanate surface: A scaling paradigm and the role of the hydrogen bond. *Phys. Chem. Chem. Phys.* **2021**, *23*, 23478.

(18) Lambert, A. G.; Davies, P. B.; Neivandt, D. J. Implementing the theory of sum frequency generation vibrational spectroscopy: A tutorial review. *Appl. Spectrosc. Rev.* **2005**, *40*, 103–145.

(19) Tian, C. S.; Shen, Y. R. Recent progress on sum-frequency spectroscopy. *Surf. Sci. Rep.* **2014**, *69*, 105–131.

(20) Buck, M.; Himmelhaus, M. Vibrational spectroscopy of interfaces by infrared–visible sum frequency generation. *J. Vac. Sci. Technol. A* **2001**, *19*, 2717–2736.

(21) Vidal, F.; Tadjeddine, A. Sum-frequency generation spectroscopy of interfaces. *Rep. Prog. Phys.* **2005**, *68*, 1095–1127.

(22) Ji, N.; Ostroverkhov, V.; Chen, C.-Y.; Shen, Y.-R. Phase-sensitive sum-frequency vibrational spectroscopy and its application to studies of interfacial alkyl chains. *J. Am. Chem. Soc.* **2007**, *129*, 10056–10057.

(23) Wei, X.; Zhuang, X.; Hong, S.-C.; Goto, T.; Shen, Y. R. Sum-frequency vibrational spectroscopic study of a rubbed polymer surface. *Phys. Rev. Lett.* **1999**, *82*, 4256–4259.

(24) Kox, T.; Spohr, E.; Kenmoe, S. Impact of Solvation on the Structure and Reactivity of the Co_3O_4 (001)/H_2O Interface: Insights From Molecular Dynamics Simulations. *Front. Energy Res.* **2020**, *8*, 312.

(25) Neugebauer, J.; Scheffler, M. Adsorbate-substrate and adsorbate-adsorbate interactions of Na and K adlayers on Al(111). *Phys. Rev. B* **1992**, *46*, 16067–16080.

(26) Kühne, T. D. et al. CP2K: An electronic structure and molecular dynamics software package - Quickstep: Efficient and accurate electronic structure calculations. *J. Chem. Phys.* **2020**, *152*, 194103.

(27) Perdew, J. P.; Burke, K.; Ernzerhof, M. Generalized gradient approximation made simple. *Phys. Rev. Lett.* **1996**, *77*, 3865–3868.

(28) Hubbard, J. Electron correlations in narrow energy bands. *Proc. R. Soc. Lond. Ser. A Math. Phys. Sci.* **1963**, *276*, 238–257.

(29) Omranpoor, A.; Kox, T.; Spohr, E.; Kenmoe, S. Influence of temperature, surface composition and electrochemical environment on 2-propanol decomposition at the Co_3O_4 (001)/H_2O interface. *Appl. Surf. Sci. Adv.* **2022**, *12*, 100319.

(30) Budiyanto, E.; Zerebecki, S.; Weidenthaler, C.; Kox, T.; Kenmoe, S.; Spohr, E.; DeBeer, S.; Rüdiger, O.; Reichenberger, S.; Barcikowski, S.; Tüysüz, H. Impact of Single-Pulse, Low-Intensity Laser Post-Processing on Structure and Activity of Mesostructured Cobalt Oxide for the Oxygen Evolution Reaction. *ACS Appl. Mater. Interfaces* **2021**, *13*, 51962–51973.

(31) Zerebecki, S. et al. Engineering of Cation Occupancy of $CoFe_2O_4$ Oxidation Catalysts by Nanosecond, Single-Pulse Laser Excitation in Water. *ChemCatChem 14*, e202101785.

(32) Zigla, A. A.; Kox, T.; Mevoa, D.; Assaouka, H. T.; Nsangou, I. N.; Daawe, D. M.; Kenmoe, S.; Kouotou, P. M. Magnesium-Modified Co_3O_4 Catalyst with Remarkable Performance for Toluene Low Temperature Deep Oxidation. *Catalysts* **2022**, *12*, 411.

(33) Kox, T.; Omranpoor, A. H.; Kenmoe, S. Structure and Reactivity of $CoFe_2O_4(001)$ Surfaces in Contact with a Thin Water Film. *PhysChem* **2022**, *2*, 321–333.

(34) Grimme, S.; Antony, J.; Ehrlich, S.; Krieg, H. A consistent and accurate ab initio parametrization of density functional dispersion correction (DFT-D) for the 94 elements H-Pu. *J. Chem. Phys.* **2010**, *132*, 154104.

(35) Yu, Y.; Wang, Y.; Hu, N.; Lin, K.; Zhou, X.; Liu, S. Overlapping spectral features and new assignment of 2-propanol in the C-H stretching region. *J. Raman Spectrosc.* **2014**, *45*, 259–265.

(36) Hansen, J. O.; Huo, P.; Martinez, U.; Lira, E.; Wei, Y. Y.; Streber, R.; Lægsgaard, E.; Hammer, B.; Wendt, S.; Besenbacher, F. Direct Evidence for Ethanol Dissociation on Rutile $TiO_2(110)$. *Phys. Rev. Lett.* **2011**, *107*, 136102.

(37) Kataoka, S.; Cremer, P. S. Probing molecular structure at interfaces for comparison with bulk solution behavior: Water/2-propanol mixtures monitored by vibrational sum frequency spectroscopy. *J. Am. Chem. Soc.* **2006**, *128*, 5516–5522.

TOC Graphic

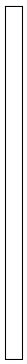

Supporting Information to *2-Propanol Interacting with Co_3O_4(001): A combined AIMD and vSFS study*

Amir H. Omranpoor, Anupam Bera, Denise Bullert, Matthias Linke, Samira Weber, Soma Salamon, Heiko Wende, Eckart Hasselbrink, Eckhard Spohr and Stéphane Kenmoe
Fakultät für Chemie and Center for Nanointegration (CENIDE), Universität Duisburg-Essen, 45117 Essen, Germany
Fakultät für Physik and Center for Nanointegration (CENIDE), Universität Duisburg-Essen, 45117 Essen, Germany

AFM Characterization Surface topography was investigated by AFM measurements, performed in air using a Bruker Dimension FastScan AFM in Bruker's PeakForce QNM imaging mode and in tapping mode. For the 1 µm x 1 µm scans the typical scan rate was 1 Hz and 512 samples per line were acquired. FastScan-A cantilevers (nom. resonant frequency: 1400 kHz, nom. spring constant: 10 N/m, nom. tip radius: 5 nm, Bruker, USA) were used. Overview scans with 5µm x 5µm were measured in PeakForce Mode, using PeakForce-HIRS-SSB cantilevers (nom. resonant frequency: 70 kHz, nom. spring constant: 0.08 N/m , nom. tip radius: 1 nm, Bruker, USA). The scan rate was 2 Hz and 1024 samples per line were acquired. Image analysis was performed using NanoScope Analysis 1.9 (Bruker, USA). The images were flattened and eventually low-pass filtered to remove high frequency noise. Generally speaking, the AFM images (Fig. S1) show a relatively flat surface topology, with no large deviations that would indicate any point or line defects, or grain boundaries, pointing towards an epitaxial growth. In addition a line scan over the surface has been depicted in Fig. S2 in comparison with support substrate MgO(001). There is no sign of typical issues often observed in samples prepared via PLD, such as droplets or particulates ejected from the target, or resputtering effects, both of which would be indicative of excessive laser fluence. Overall, the AFM results indicate that the chosen parameters for the sample deposition and subsequent annealing are suitable to obtain a single crystalline Co_3O_4 film.

XRD Characterization X-ray diffractograms were recorded at room temperature with a Philips PW1730 using a Cu K-alpha anode in 2-theta steps of 0.02°. The resulting diffractogram displays strong main peaks of the MgO substrate, as well as of the desired Co_3O_4 sample layer, as visible by comparison to mineral database peak positions. A general broadening of the absorption lines can be seen, usually originating from the substrate, which is further exacerbated by the low thickness of the sample layer. No significant traces of parasitic phases can be detected, apart from minute contributions of CoO, representing an off-stoichiometric fraction of the original target material.

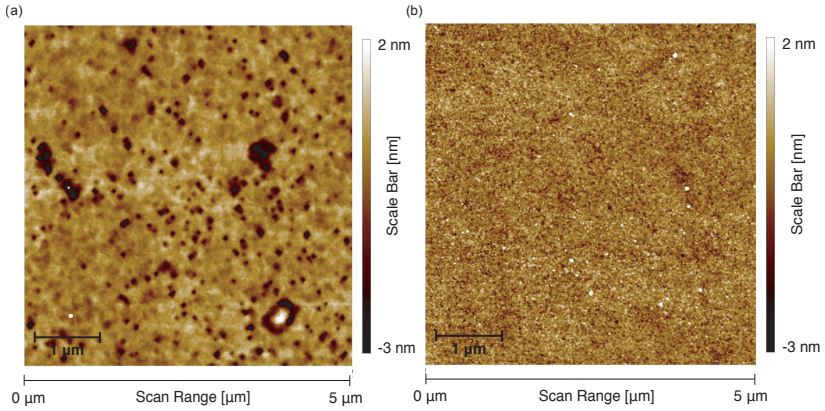

FIGURE S1. (a) AFM topography obtained for $Co_3O_4(001)/MgO(001)$ thin film and (b) MgO(001) reference substrate.

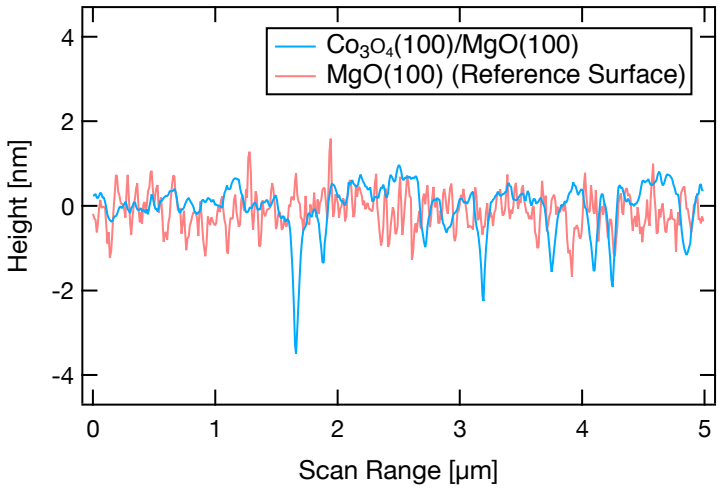

FIGURE S2. Typical line profile across the AFM image (Fig. S1) of a $Co_3O_4(001)/MgO(001)$ thin film in comparison to one recorded for the bare MgO(001) reference substrate.

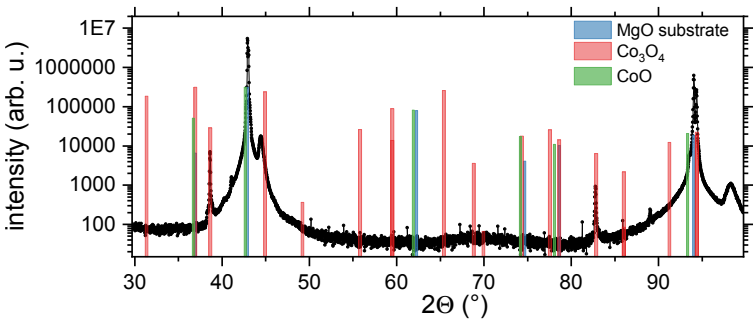

FIGURE S3. Typical XRD image of the used 150 nm thin $Co_3O_4(001)$ films deposited on MgO(001).

Spectral Analysis The non-resonant signal from the bare Co_3O_4 on Mg(001) sample when using the *ppp* polarization combination was recorded for various temperatures. It is found to consistently shows some broad structure.

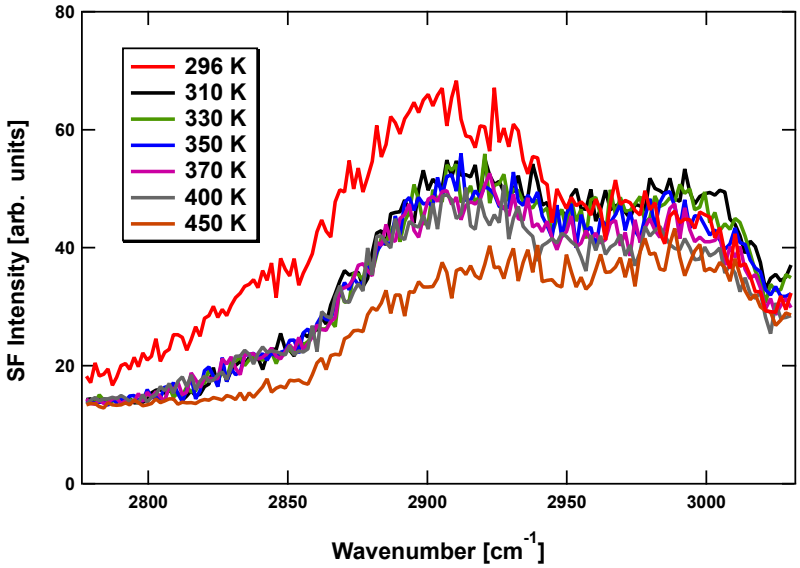

FIGURE S4. Non-resonant sum frequency response of the 150 nm Co_3O_4(001) on MgO(001) sample used for various temperatures (*ppp*).

Fitting parameters to the vSF spectra

For the fit to the *pp* spectrum a wavenumber dependent function was used derived by smoothing the 450 K data displayed in Fig. S4.

Offset: 3.80E-02	Non-res Bg: 0.95			
Label	Wavenumber	A [arb. u.]	Γ	ϕ
ν_{CH}	2850	0.088	11.5	-2.65*
ν_{CH}	2874	0.21	11.5	-2.65*
r^+	2884	0.458	12.0	3.89**
ν_{CH}	2901	0.446	11.5	-2.65*
ν_{CH}	2925	0.259	11.5	-2.65*
r^+_{FR}	2944	0.559	10.0	3.89**
r^-	2978	0.682	9.0	-2.71

TABLE S1. Fitting parameters: *ppp*

* These positions of the 4 modes were inferred from previous fits to spectra of 2-propanol-d6 on TiO_2. Moreover, the ratio between the A values was also taken from that work. The 4 phases were forced to have a common value.
** The phases of these two CH_3 symmetric modes were forced to share one value.

Offset: 2.57E-02	Non-res Bg: 0.067			
Label	Wavenumber	Γ [arb. u.]	Γ	ϕ
ν_{CH}	2850	0.225	10.0	0.12*
ν_{CH}	2872	0.192	20.0	0.12*
r^+	2884	0.593	12.5	-0.30*
ν_{CH}	2903	0.287	10.0	0.12*
ν_{CH}	2926	0.225	10.0	0.12*
r^+_{FR}	2944	0.722	12.5	-0.30*

TABLE S2. Fitting parameters: *ssp*

* The phases were represented by a a pair of fitting parameter, one for teh symmetric and one for the methine modes.

Offset: 2.50E-02	Non-res Bg: 0.145			
Label	Wavenumber	A [arb. u.]	Γ	ϕ
r^-	2980	0.287	9.3	-1.47

TABLE S3. Fitting parameters: *sps*

TABLE S4. Compilation of the optical parameters used.

λ [nm]	461 (SF)	532 (vis)	3450 (IR)
$n_{Co_3O_4}$ [7]	2.85 + 0.4i	2.7 + 0.35i	2.6 (2.4 - 2.85)
n (air)	1	1	1
n_{MgF_2}	1.43 [6]	1.42 [6]	1.37 [2]

Orientational Analysis A detailed description of orientational analysis is given elsewhere [1]. In short, we fitted the spectra to $\left|\left|\chi^{(2)}_{NR}\right| + \sum_i e^{i\xi_i} \frac{A_i}{\omega_{IR}-\omega_i+i\Gamma_i}\right|^2$ after correcting the *ssp* and *sps* spectra by factors of 1.98 and 1.67 with respect to the *ppp*-spectrum to account for the lower transmitted power of *s*-polarized light when passing through the MgF_2 window. The refractive indices can be found in Tab. S4. While the refractive indices of Co_3O_4 for the wavelengths of the SF and vis beams can be found in the literature [7], to the best of our knowledge there are no values for the mid-IR range in the literature. For this reason we look at a range of possible refractive indices. We restrict the upper limit to 2.85, since the refractive index in the IR is generally lower than in the vis. We set the lower limit to 2.4 corresponding to the value for CoO systems which generally have a lower refractive index than Co_3O_4 systems [4]. We will show that letting the refractive index range between those values will only slightly alter the extracted angles while increasing the error margins slightly. As a reference point we choose the refractive index to be 2.6.

To calculate the orientation of the molecule, we assumed an azimuthally isotropic surface and followed Kataoka's and Cremer's united atom approach[5, 3], which treats the isopropyl moiety as a whole. We set the C-C-C bond angle between the two methyl groups to 112°. Since the group's symmetry axis, the vector bisecting the two methyl groups, does not necessarily align with the surface normal, the twist angle, i.e. the rotation around it, cannot be averaged out. As a result, an infinite number of possible pairs of twist and tilt angles can be assessed to the experimentally obtained intensity ratio. To overcome this problem, we obtain the orientation of the methine group, which then constricts the orientation of the isopropyl group to an exact pair of Euler angles with reasonable margins of error. We derive this information for the methine group using the method described by Wang *et al.* [8], namely from the intensity ratio of the CH mode observed in the *ssp* and *ppp* spectrum. The C-H bond's tilt angle with respect to the surface normal is calculated as $103 \pm 1°$, which in turn restricts the isopropyl group's tilt angle to be $37 \pm 2°$ and the twist angle to be $29 \pm 3°$, after setting the angle between the methine group and the bisecting isopropyl vector to 125°. Assuming a H−C−O bond angle of 110°, the CO vector's tilt angle is calculated as 154° with respect to the surface normal, i.e. the CO bond is pointing towards the surface [5, 3].

Allowing the refractive index of Co_3O_4 to range between 2.4 and 2.85 results in values for the tilt angle of $37 \pm 4°$ and the twist angle of $29 \pm 4°$ for the isopropyl group. It should be noted that we follow the convention such that a twist angle of 90° corresponds to the two methyl groups being equidistant from the surface plane.

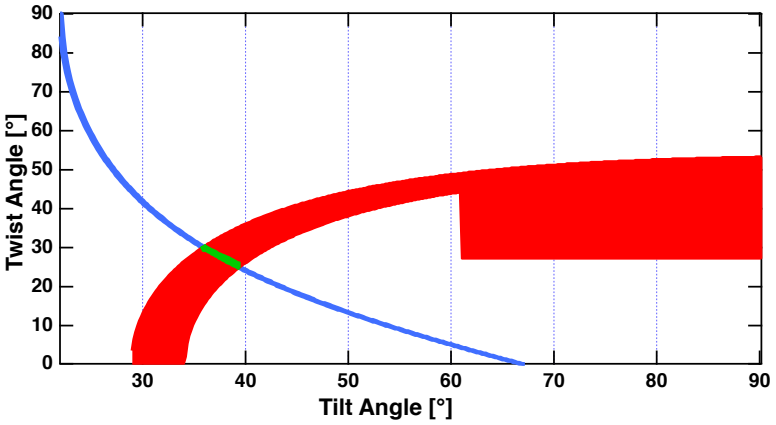

FIGURE S5. Combinations of twist and tilt angles of the isopropyl group as extracted from the CH_3-as stretching (red) and geometrical restrictions to them based on the methine CH intensity ratio (blue) between the *ssp* and *ppp* spectra. The overlap of both areas (green) represents the possible combination of twist and tilt angles of the isopropyl group consistent with both experiments.

[1] Anupam Bera et al. "Vibrational Sum Frequency Spectroscopy Study of Alcohol Adsorption on Thin-Film TiO_2 at Ambient Pressure and Temperature". In: *J. Phys. Chem. C* 125.14 (2021), pp. 7721–7727.

[2] Marilyn J Dodge. "Refractive properties of magnesium fluoride". In: *Appl. Opt.* 23.12 (1984), pp. 1980–1985. DOI: 10.1364/AO.23.001980.

[3] Benjamin Doughty et al. "Absolute molecular orientation of isopropanol at Ceria(100) surfaces: Insight into catalytic selectivity from the interfacial structure". In: *J. Phys. Chem. C* 121 (2017), pp. 14137–14146. DOI: 10.1021/acs.jpcc.7b03272.

[4] Danick Gallant, Michel Pezolet, and Stephan Simard. "Optical and physical properties of cobalt oxide films electrogenerated in bicarbonate aqueous media". In: *J. Phys. Chem. B* 110.13 (2006), pp. 6871–6880.

[5] Sho Kataoka and Paul S. Cremer. "Probing molecular structure at interfaces for comparison with bulk solution behavior: Water/2-propanol mixtures monitored by vibrational sum frequency spectroscopy". In: *J. Am. Chem. Soc.* 128.16 (2006), pp. 5516–5522. DOI: 10.1021/ja060156k.

[6] Luis V Rodrıguez-de Marcos et al. "Self-consistent optical constants of MgF_2, LaF_3, and CeF_3 films". In: *Opt. Mater. Express* 7.3 (2017), pp. 989–1006. DOI: 10.1364/OME.7.000989.

[7] A. J. Varkey and A. F. Fort. "A chemical method for preparation of cobalt oxide thin films". In: *Solar energy materials and solar cells* 31.2 (1993), pp. 277–282. DOI: 10.1016/0927-0248(93)90058-B. URL: https://doi.org/10.1016/0927-0248(93)90058-B.

[8] Hong-Fei Wang et al. "Quantitative spectral and orientational analysis in surface sum frequency generation vibrational spectroscopy (SFG-VS)". In: *Int. Rev. Phys. Chem.* 24 (2005), pp. 191–256. DOI: 10.1080/01442350500225894.